Thermal behavior of SMA/FGM actuators with temperature dependent properties

Ali Talezadeh Lari, Ali Nikbakht, and Mojtaba Sadighi

New Technologies Research Center (NTRC), Amirkabir University of Technology, Tehran, Iran

ABSTRACT: In the present study, a semi-analytical solution is introduced to analyze the non-linear thermal stability of a laminated composite box actuator or sensor beam, consisted of a functionally graded core with shape memory alloy bonding layer faces with uniform rectangular cross sections. The analysis is based on the first-order shear deformation theory which incorporates the transverse shear deformation. Additionally, the geometrical non-linearity is included in the von-Karman sense. The elastic material properties of the graded material are considered to be temperature dependent. The effect of materials properties distribution in the graded layer, the activation temperature and the thickness of the graded layer is investigated. The results show that the presence of the shape memory alloy in the structure, even in the form of thin layers can magnificently reduce the deflection. In general, SMA/FGM actuators or sensors have smaller deflections compared to functionally graded actuators.

1 INTRODUCTION

In the present challenge of developing lightweight and highly performing flexible structures, the concepts of self-controlling and self-monitoring capabilities possess high level of importance. These capabilities are achieved by taking advantage of the properties of smart materials in the form of actuators and sensors, embedded and distributed inside the structure. In a smart structure, the thermo-mechanical loading inserted on the structure is used as the triggering factor of the self-controlling and self-monitoring behavior of these actuators and sensors. On the other hand, the actuator or sensor itself should sustain this thermal loading condition while keeping its functionality. Following the goal of having high strength-to-weight and stiffness-to-weight ratios and also tolerating sever thermal loadings, brings the idea of utilizing functionally graded materials (FGMs) or shape memory alloys (SMAs) or a combination of both into a designer's mind.

FGMs are a class of composites that has a smooth and continuous variation of material properties from one surface to another and thus can alleviate stress concentrations found in laminated composites. Many researchers have worked on linear and nonlinear deformation, instability and vibration of structures made of FGMs.

On the other hand, in many practical cases, the above explained actuator or sensor may be modeled by a beam with specified boundary conditions. In this case, due to sever loading condition, a realistic assumption is to consider nonlinear deformation of the modeled beam. Many researches have been conducted on nonlinear deformation of FG beams. Some examples are as follows. Li et al. (2006) studied thermal post-buckling of Timoshenko FG beams. Ke et al. (2010) studied nonlinear vibration of functionally graded (FG) beams made, based on Euler-Bernoulli beam theory and von Karman geometric nonlinearity. Ma and Lee (2012) gave an exact solution for nonlinear static response of a shear deformable FG beam under an in-plane thermal loading.

SMAs have been receiving increased attention owing to their unique thermo-mechanical properties such as shape memory behavior and pseudo-elasticity deformation. The origin of SMA features is a reversible martensitic phase transformation. These unique properties have made SMAs as a major intelligent material in many practical engineering fields. However, the quest of developing lightweight has led the designers to take advantage shape memory alloy hybrid composite (SMAHC). When SMAHCs are heated, the SMA fibers are prevented from recovering their initial strains by matrix medium. This restriction induces large tensile stress (recovery stress) inside the structure. The generated recovery stress has a significant effect on the structure characteristics and can be utilized to achieve vibration control, structural reinforcement and shape change (refer to Lagoudas (2008)). Based on this interesting behavior, Choi et al. (1999) performed an experimental study on active buckling control of SMAHC beams. Their experimental results revealed that SMA wires can be used for the buckling control of laminated composite beams which are subjected to mechanical loading and then exposed to an elevated temperature which influences phase transformation of SMA wires. Zhang et al. (2006) have presented the vibrational behavior of laminated composite plates containing unidirectional fine SMA wires and woven SMA layer by experiments. Yongsheng and Shuangshuang (2007) investigated large amplitude flexural vibration of the orthotropic composite plate with embedded SMA fibers using the Galerkin approximate and harmonic balance methods. Buckling analysis of SMA reinforced composite laminates was studied by Kuo et al. (2009) employing FE method and approximate data from the SMA curves. Mirzaeifar et al. (2011) presented a semi analytical analysis of shape memory alloy thick-walled cylinders under internal pressure.

As mentioned, a combination of FGMs and SMAs properties in actuators or sensors could be considered as a novel idea in the field of self-monitoring and self-controlling smart structures. The linear problem has been studied by Sepiani et al. (2009). In spite of the accompanied complexity of the analysis, a non-linear analysis of the SMA/FGM actuator or sensor seems to be necessary due to the large deformations which occur with the displacements of a structure.

In the present study, a semi-analytical solution is introduced to analyze the non-linear thermal stability of a laminated composite actuator or sensor. The actuatuor or sensor is modeled by a composite beam consisted of an FGM core with SMA bonding layer faces with a uniform rectangular cross section. The analysis is based on the first-order shear deformation theory which incorporates the geometrical nonlinearity as von-Karman strain components. The elastic material properties of the FGM are considered to be temperature dependent and the nonlinear phase transformation kinetics proposed by Lin and Rogers (1991) is utilized to calculate the recovery stress induced by the martensitic phase transformation of the prestrained SMA components. The effect of materials properties distribution in the FG layer, the activation temperature and the slenderness ratio of the FG layer are investigated.

2 ELASTIC PROBLEM FORMULATION

The geometry of the SMA/FGM beam under consideration is shown in Figure 1, where the thicknesses of SMA faces are assumed to be equal (h_s).

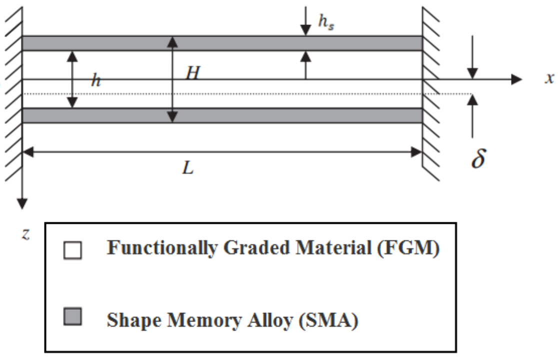

Figure 1. The geometry of the considered problem.

The graded material is usually consisted of a ceramic and a metal phase, which are denoted in the formulation by c and m indices, respectively. The thermal and mechanical properties of the FG section of the beam are calculated by the linear rule of mixtures as follows:

$$\begin{pmatrix} E_f(z) \\ \rho_f(z) \\ \alpha_f(z) \\ k_f(z) \end{pmatrix} = \begin{pmatrix} E_c - E_m \\ \rho_c - \rho_m \\ \alpha_c - \alpha_m \\ k_c - k_m \end{pmatrix} V_c + \begin{pmatrix} E_m \\ \rho_m \\ \alpha_m \\ k_m \end{pmatrix} \tag{1}$$

where the index f refers to the property of the FG material. In this equation E, ρ, α and k are the modulus of elasticity, density, coefficient of thermal expansion and thermal conductivity, respectively, and V_c is the volume fraction of the ceramic phase. A symmetric distribution of the ceramic phase is assumed through the thickness of the FG section which is given by the following relation:

$$V_c(z) = \begin{cases} (1 - 2z/h)^n & 0 \le z \le h/2 \\ (1 + 2z/h)^n & -h/2 \le z \le 0 \end{cases} \tag{2}$$

In this equation, z is the coordinate through the thickness of the beam and n is the exponent that defines the way in which the material properties change in the graded medium. Since thermal loading is acting on the beam and with the goal of creating more realistic results, the modulus of elasticity of the graded section is considered to be temperature dependant. The dependency on the temperature is estimated as

$$E_j = E_j^0 \left(E_j^{-1} T^{-1} + 1 + E_j^1 T + E_j^2 T^2 + E_j^3 T^3 \right), \quad j: c \ or \ m \tag{3}$$

where E_j^i $(i = -1,0,1,2,3)$ are material constants which values may be found in text books for any material (refer to Shen, 2009).

In the SMA layers, the modulus of elasticity is written as

$$E_i = \zeta_i E_M + (1 - \zeta_i) E_A, \quad i = 1,3 \tag{4}$$

In this equation, the indices 1 and 3 denote the SMA face layers at the upper and lower surfaces of the beam, respectively. The smart behavior of shape memory alloys depend on the phase transformation of Austenite to Martensite and vice versa. In Equation 4, E_A and E_M denote the modulus of elasticity of Austenite and Martensite, respectively. ζ_i (i: 1 and 3) is the volume fraction of the Martensite in the corresponding SMA layer. This volume fraction is a function of temperature. There are several models by which the mathematical representation of the Martensite volume fraction and its dependency on temperature may be found. In this study, the linear model of Lin and Rogers (1991) is assumed:

$$\zeta_i = \begin{cases} 1 & T \le A_s + |\sigma|/C_A \\ 1 - \frac{T-A_s}{A_f-A_s} + \frac{|\sigma|}{C_A(A_f-A_s)} & A_s + |\sigma|/C_A \le T \le A_f + |\sigma|/C_A \\ 0 & A_f + |\sigma|/C_A \le T \end{cases} \tag{5}$$

where A_s and A_f represent austenite start and austenite final temperatures, respectively, and C_A is the stress-temperature slope for austenite start temperature diagram. In general, for the graded section the stress-strain relation is written as:

$$\sigma_x = E_f(\varepsilon_x - \alpha_f \Delta T) \tag{6}$$

and this relation in the SMA layers takes the following format:

$$\sigma_x = E_s e + \theta \Delta T + \Omega(\zeta - 1) \tag{7}$$

In these relations, $\Delta T = \Delta T(z) = T - T_0$ (T_0 is the initial temperature of the beam) is the temperature gradient at each point of the beam. In Equation 7, E_s is the modulus of elasticity of the SMA layer, $e = \varepsilon - \varepsilon_r$ is the relative strain in this layer, θ and Ω are the thermal and the phase transformation moduli of the smart material, respectively. The temperature distribution in the beam, $T(\mathrm{z})$, is obtained by solving the thermal conduction relation:

$$\frac{\mathrm{d}}{\mathrm{d}z}\left(k(z)\frac{\mathrm{d}T(z)}{\mathrm{d}z}\right) = 0 \tag{8}$$

The thermal boundary conditions of the problem are as follows

$$\begin{aligned} T(z) &= T_1, \quad z = H/2 \\ T(z) &= T_3, \quad z = -H/2 \end{aligned} \tag{9}$$

where T_1 and T_3 are the temperature at the upper and lower surfaces of the beam, respectively. In fact, these temperatures control the deformation of the beam. Here, the SMA layers are assumed to be so thin that the temperature gradient vanishes through their thickness. The solution of Equation 9 is written as follows:

$$\begin{aligned} T_2(z) = T_3 + \frac{T_1-T_3}{C}\Bigg[\left(\frac{2z+h}{2h}\right) - \frac{(k_c-k_m)}{(n+1)k_m}\left(\frac{2z+h}{2h}\right)^{n+1} + \frac{(k_c-k_m)^2}{(2n+1){k_m}^2}\left(\frac{2z+h}{2h}\right)^{2n+1} - \\ \frac{(k_c-k_m)^3}{(3n+1){k_m}^3}\left(\frac{2z+h}{2h}\right)^{3n+1} + \frac{(k_c-k_m)^4}{(4n+1){k_m}^4}\left(\frac{2z+h}{2h}\right)^{4n+1} - \frac{(k_c-k_m)^5}{(5n+1){k_m}^5}\left(\frac{2z+h}{2h}\right)^{5n+1}\Bigg] \end{aligned} \tag{10}$$

In which

$$C = 1 - \frac{(k_c-k_m)}{(n+1)k_m} + \frac{(k_c-k_m)^2}{(2n+1){k_m}^2} - \frac{(k_c-k_m)^3}{(3n+1){k_m}^3} + \frac{(k_c-k_m)^4}{(4n+1){k_m}^4} - \frac{(k_c-k_m)^5}{(5n+1){k_m}^5} \tag{11}$$

In order to solve the problem, a physical neutral surface is assumed at $z = \delta$. The value of δ is defined such that the stretch-bending coupling in the beam vanishes. Based on this assumption, the strain-displacement relation may be written as

$$\varepsilon_x = u_{,x} + \frac{1}{2}w_{,x}^2 - (z-\delta)w_{,xx} \tag{12}$$

where u and w are the displacement components at the physical neutral surface in x and z directions, respectively. The resultant force (N) and moment (M) are equal to

$$\begin{pmatrix} N \\ M \end{pmatrix} = \int_{-H/2}^{H/2} \begin{pmatrix} \sigma_x \\ \sigma_x.(z-\delta) \end{pmatrix} \mathrm{d}z = \begin{pmatrix} A & B \\ B & D \end{pmatrix} \begin{pmatrix} u_{,x} + \frac{1}{2}{w_{,x}}^2 \\ -w_{,xx} \end{pmatrix} - \begin{pmatrix} N^T \\ M^T \end{pmatrix} - \begin{pmatrix} N^P \\ M^P \end{pmatrix} \tag{13}$$

The superscripts T and P refer to the terms which are caused by thermo-elastic and shape memory induced stresses, respectively. The values of A, B and D are given by the following equation:

$$\begin{pmatrix} A \\ B \\ D \end{pmatrix} = \int_{-H/2}^{H/2} \begin{pmatrix} 1 \\ (z-\delta) \\ (z-\delta)^2 \end{pmatrix} E\mathrm{d}z \tag{14}$$

As mentioned, the position of the neutral physical surface is found hypothetically by omitting the stretch-bending coupling, which is the case of $B = 0$. Thus the value of δ is equal to

$$\delta = \int_{-H/2}^{H/2} zE\mathrm{d}z \Big/ \int_{-H/2}^{H/2} E\mathrm{d}z \tag{15}$$

The thermo-elastic and shape memory stress induced terms in the resultant force and moment of Equation 13 are

$$\begin{aligned} N^T &= \int_{-\frac{H}{2}}^{-\frac{h}{2}} -\theta\Delta T_1 \mathrm{d}z + \int_{-\frac{h}{2}}^{\frac{h}{2}} E_f \alpha_f \Delta T_2 \mathrm{d}z + \int_{\frac{h}{2}}^{\frac{H}{2}} -\theta \Delta T_3 \mathrm{d}z \\ M^T &= \int_{-\frac{H}{2}}^{-\frac{h}{2}} -\theta\Delta T_1 (z-\delta)\mathrm{d}z + \int_{-\frac{h}{2}}^{\frac{h}{2}} E_f \alpha_f \Delta T_2 (z-\delta)\mathrm{d}z + \int_{\frac{h}{2}}^{\frac{H}{2}} -\theta\Delta T_3 (z-\delta)\mathrm{d}z \\ N^P &= \int_{-\frac{H}{2}}^{-\frac{h}{2}} \Omega(1-\zeta_1)dz + \int_{\frac{h}{2}}^{\frac{H}{2}} \Omega(1-\zeta_3)\mathrm{d}z \\ M^P &= \int_{-H/2}^{-h/2} \Omega(1-\zeta_1)(z-\delta)\mathrm{d}z + \int_{h/2}^{H/2} \Omega(1-\zeta_3)(z-\delta)\mathrm{d}z \end{aligned} \tag{16}$$

Replacing Equation 5 into the third and fourth relations of Equation 16 results in the following relations for N^P and M^P

$$\begin{aligned} N^P =& \frac{-\mathrm{sgn}(\sigma)(E_1 h_1 + E_3 h_3)\Omega}{C_A(A_f - A_s) - \mathrm{sgn}(\sigma)\Omega} u_{,x} + \frac{-\mathrm{sgn}(\sigma)(E_1 L_1 + E_3 L_3)\Omega}{C_A(A_f - A_s) - \mathrm{sgn}(\sigma)\Omega} w_{,x} \\ &+ \frac{C_A[T_1 + T_3 - 2A_s - \mathrm{sgn}(\sigma)\theta(\Delta T_1 + \Delta T_3)]h_1\Omega}{C_A(A_f - A_s) - \mathrm{sgn}(\sigma)\Omega} + \Omega(h_1 + h_3) \\ M^P =& \frac{-\mathrm{sgn}(\sigma)(E_1 L_1 + E_3 L_3)\Omega}{C_A(A_f - A_s) - \mathrm{sgn}(\sigma)\Omega} u_{,x} + \frac{-\mathrm{sgn}(\sigma)(E_1 I_1 + E_3 I_3)\Omega}{C_A(A_f - A_s) - \mathrm{sgn}(\sigma)\Omega} w_{,x} \\ &+ \frac{C_A[T_1 + T_3 - 2A_s - \mathrm{sgn}(\sigma)\theta(\Delta T_1 + \Delta T_3)]L_1\Omega}{C_A(A_f - A_s) - \mathrm{sgn}(\sigma)\Omega} + \Omega(L_1 + L_3) \end{aligned} \tag{17}$$

In which

$$L_1 = \int_{\frac{h}{2}}^{\frac{H}{2}} (z-\delta)dz, \quad L_3 = \int_{\frac{-H}{2}}^{\frac{-h}{2}} (z-\delta)dz$$
$$I_1 = \int_{\frac{h}{2}}^{\frac{H}{2}} (z-\delta)^2 dz, \quad I_3 = \int_{\frac{-H}{2}}^{\frac{-h}{2}} (z-\delta)^2 dz \tag{18}$$

Based on Hamilton's principle, the equations of equilibrium of the beam are

$$N_{,x} = 0$$
$$(N.w_{,x})_{,x} + M_{,xx} + q = 0 \tag{19}$$

Since there is no external mechanical loading, $q = 0$. The first relation of Equation 19 implies that the resultant force is a constant through the beam, thus the following equation may be obtained:

$$N = const = A\left(u_{,x} + \frac{1}{2}{w_{,x}}^2\right) - N^T - N^P \tag{20}$$

Here, the beam is assumed to be clamped at both ends. Therefore, the geometrical boundary conditions are:

$$x = 0, L \quad \rightarrow \quad w = 0, w_{,x} = 0$$
$$x = 0, L \quad \rightarrow \quad u = 0 \tag{21}$$

By considering Equation 17, Equation 20 may be rewritten as

$$N = \frac{\mathrm{A} - \Lambda}{2\mathrm{L}} \int_0^{\mathrm{L}} \left({\mathrm{w}_{,x}}^2\right) \mathrm{dx} - \left(\mathrm{N}^{\mathrm{T}} + \Gamma\right) \tag{22}$$

where

$$\Lambda = (-sgn(\sigma)(E_1h_1 + E_3h_3)\Omega)/\left(C_A\left(A_f - A_s\right) - sgn(\sigma)\Omega\right)$$
$$\Gamma = (C_A[T_1 + T_3 - 2A_s - sgn(\sigma)\theta(\Delta T_1 + \Delta T_3)]L_1\Omega)/\left(C_A\left(A_f - A_s\right) - sgn(\sigma)\Omega\right) \tag{23}$$

In general, the solution of the problem is based on finding the displacement components, u and w. If u were not present in Equation 20, the second relation of Equation 19 could be solved by an exact mathematical procedure and a closed form solution could be obtained for w. This may have been done by replacing N from Equation 22 into the second relation of Equation 19. However, in this case (nonlinear SMA/FGM beam), two equations should be available to obtain u and w simultaneously. These two equations are the equilibrium equations given in Equation 19. To the furthest knowledge of the authors, there is no exact solution for this problem. Thus here, these equations are solved numerically by means of nonlinear GDQ method and the results are presented in the next section.

3 RESULTS AND DISCUSSION

The material properties which are assumed in the analysis are listed in Tables 1 and 2 for FG and SMA layers, respectively (extracted from Brinson 1993 and Sepiani et al. 2009). The results for the dimensionless critical thermal buckling load based on a shooting method presented by Ma and Lee (2011) are compared with the corresponding results obtained here (Figure 2). The close match between the results verifies the procedure used in this paper.

Table 1. Material properties of the FGM core beam.

$E_c\ (GPa)$	$E_m\ (GPa)$	$\rho_c\ (kg/m^3)$	$\rho_m\ (kg/m^3)$	Poisson's Ratio
205	70	8900	7000	0.3

Table 2. Material properties for a Nitinol alloy, extracted from Brinson (1993).

Module/Density	Transformation Temperatures	Transformation Constants	Others	
$E_a = 67 \times 103\, MPa$	$M_f = 9$ °C	$C_M = 8\ MPa/$°C	Max. Residual Strain	$\varepsilon_L = 0.067$
$E_m = 26.3 \times 103\, MPa$	$M_s = 18.4$ °C	$C_A = 13.8\ MPa/$°C	Resistivity	$\rho_e = 0.9 \times 10^{-6}$
$\theta = 0.55\ MPa/$°C	$A_f = 49$ °C	$\sigma_s^{cr} = 100\, MPa$	Specific heat	$C_p = 920\ J/kg$°C
$\rho = 6500\ kg/m^3$	$A_s = 34.5$ °C	$\sigma_f^{cr} = 170\, MPa$	Conductivity	$\chi = 18\ W/m$°C

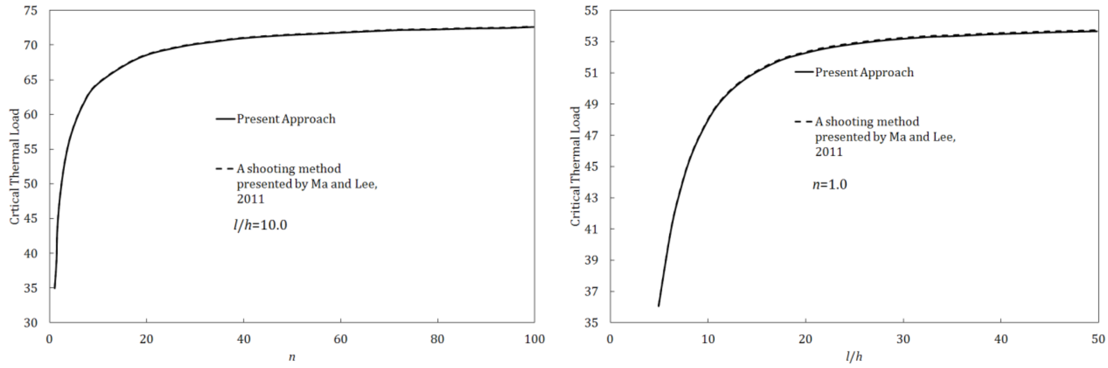

Figure 2. Comparison of the present approach for the critical thermal buckling load of a clamped-clamped SMA/FGM beam with numerical results obtained by a shooting method ($h_1 = h_2 = 0.05h$).

The post-buckling paths of an FGM beam and an SMA/FGM beam are compared in Figure 3. As it can be seen in this figure, for an FGM beam without SMA face layers, the deflection of the beam increases as n is increased. This is due to the fact that increasing n is equal to increasing the total volume fraction of the metal phase in the beam which leads to a softening in the overall elastic properties. This softening causes higher deflections. The results show that if SMA faces are added to the beam, the deflection reduces drastically. This is shown in Figure 3 with the solid line without marker. This line demonstrates the case in which $n = 1$ and $h_1 = h_2 = 0.05h$. It is deduced form this figure that even very thin layers of SMA can have enormous effects on the deflection. The effect of changing material properties distribution on the post-buckling of SMA/FGM beams is similar to FGM beams and the trend of the curves are the same when n is increased in SMA/FGM beams.

The effect of l/h is also demonstrated in Figure 3. The results of this figure state that changing the value of l/h does not greatly affect the deflection of an FGM beam; however, in SMA/FGM beams varying this value greatly affects the results.

4 CONCLUSIONS

In this paper, thermal post-buckling of a clamped-clamped SMA/FGM beam is investigated. The results show that even very thin layers of SMA can enormously affect the deflection of the beam. For similar material properties distribution, SMA/FGM beams have smaller deflections compared to FGM beams. In addition, while slenderness ratio does not affect the post-buckling behavior of FGM beams that much, this ratio enormously changes the deflection of SMA/FGM beams.

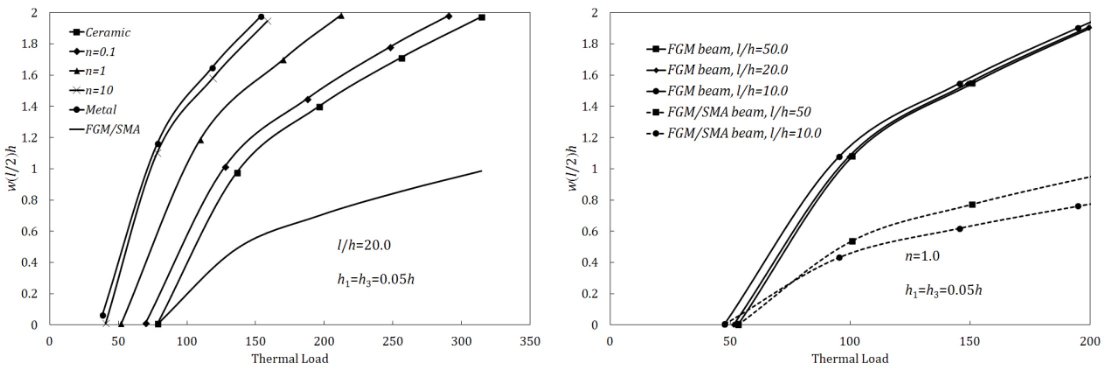

Figure 3. (Left) The effect of changing material properties distribution on the post-buckling paths of FGM and SMA/FGM clamped-clamped beams; $n = 1$ for the SMA/FGM beam. (Right) The effect of changing l/h on the post-buckling paths of FGM and SMA/FGM clamped-clamped beams; $n = 1$.

5 REFERENCES

Brinson, L.C., 1993, One dimensional constitutive behavior of shape memory alloys: thermo-mechanical derivation with non-constant material functions. *Journal of Intelligent Material Systems and* Structures, 4(2): 229-242.

Choi, S., J.J. Lee, D.C. Seo, and S.W. Choi, 1999, The active buckling control of laminated composite beams with embedded shape memory alloy wires. *Composite Structures*, 47: 679-686.

Ke, L.L., J. Yang, and S. Kitipornchai, 2010, An analytical study on the nonlinear vibration of functionally graded beams. *Meccanica*, 45: 743-752.

Kuo, S.Y., L.C. Shiau, and K.H. Chen, 2009, Buckling analysis of shape memory alloy reinforced composite laminates, *Composite Structures*, 90: 188-195.

Lagoudas, D.C. 2008. *Shape Memory Alloys: Modeling and Engineering Applications*. New York: Springer.

Li, S.R., J.H. Zhang, and Y.G. Zhao, 2006, Thermal post-buckling of functionally graded material Timoshenko beams. *Applied Mathematical Mechanics*, 27: 803-810.

Lin, M.W., and C.A. Rogers, 1991, Analysis of stress distribution in a shape memory alloy composite beam. *AIAA*, Paper-91-1164.

Ma, L.S., D.W. Lee, 2011, A further discussion of nonlinear mechanical behavior for FGM beams under in-plane thermal loading. *Composite Structures*, 93: 831-842.

Ma, L.S., and D.W. Lee, 2012, Exact solutions for nonlinear static responses of a shear deformable FGM beam under an inplane thermal loading. *European Journal of Mechanics A/Solids*, 31: 13-20.

Mirzaeifar, R., M. Shakeri, R. DesRoches, and A. Yavari, 2011, A semi-analytic analysis of shape memory alloy thick-walled cylinders under internal pressure. *Archive of Applied Mechanics*, 81: 1093-1116.

Sepiani, H., F. Ebrahimi, and H. Karimipour, 2009, A mathematical model for smart functionally graded beam integrated with shape memory alloy actuators. *Journal of Mechanical Science and Technology*, 23: 3179-3190.

Shen, H.S. 2009. *Functionally Graded Materials: Nonlinear Analysis of Plates and Shells*. Boca Raton: Taylor & Francis Group.

Yongsheng, R., and S. Shuangshuang, 2007, Large amplitude flexural vibration of the orthotropic composite plate embedded with shape memory alloy fibers. *Chinese Journal of Aeronautics*, 20: 415-424.

Zhang, R.X., Q.Q. Ni, A. Masuda, T. Yamamura,and M. Iwamoto, 2006, Vibration characteristics of laminated composite plates with embedded shape memory alloys. *Composite Structures*, 74: 389-398.